20. (a) Evans, D. J.; Hoover, W. G.; Failor, B. H.; Moran, B.; Ladd, A. J. C. *Phys. Rev.* **1988**, A. *28*, 1016. (b) Simmons, A. D.; Cummings, P. T. *Chem. Phys. Lett.* **1986**, *129*, 92.
21. Gear, W. C. *Numerical Initial Value Problems in Ordinary Differential Equations*; McGraw-Hill, New York, 1965.
22. Bareman, J. P.; Klein, M. L. *J. Phys. Chem.* **1990**, *94*, 5202.

Fluorescence and Laser Light Scattering Studies of Modified Poly(ethylene-*co*-methylacrylate) Ionomers on the Formation of Stable Colloidal Nanoparticles in Aqueous Solution

Sang-Ihn Yeo and Kyu Whan Woo*

Department of Chemistry Education, Seoul National University, Seoul 151-742, Korea
Received May 1, 1998

Fluorescence and dynamic light scattering measurements were applied to the study of formation and structure of aggregated colloidal particles in modified poly(ethylene-*co*-methylacrylate) ionomers in aqueous solution. Both 8-anillino-1-naphthalene-sulfonic acid (ANS) and pyrene were used as fluorescence probe to obtain the information on the structure of particle surface and inside, respectively. Three different ionomers used in this study started to aggregate at very dilute concentration, $3\text{-}8\times10^{-6}$ g/mL. In this study, we demonstrate that the polyethylene ionomers can form stable nanoparticles. The hydrophobic core made of the polyethylene backbone chains is stabilized by the ionic groups on the particle surface. Such a formed stable nanoparticles have a relatively narrow size distribution with an average radius in the range of 27-48 nm, depending on the kind of ionic groups. Once the stable particles are formed, the particle size distributions were nearly constant. This study shows another way to prepare surfactant-free polyethylene nanoparticles.

Introduction

Currently the term ionomer applies to a much larger category of polymers that is made up primarily of non-polar repeating units, with a small percentage of salt-containing units.[1-2] Most common non-polar comonomers used are ethylene and styrene. More than 30 years after the introduction of Surlyn® by DuPont, an intense research effort has been devoted to ionomers. Recently for environment reasons, attention has been focused on polymers that can be used in water-based formulations. The association/dissociation of ionomers in nonpolar and polar solvents have been a focused issue for more than 10 years, and the lightly sulfonated polystyrene ionomer was usually chosen as a model compound.[3] In nonpolar solvent, such as tetrahydrofuran (THF) and xylene, the ionic groups are not completely dissociated, but exist as solvated ion-pairs. Consequently these lead to the association of ionomers, which has been experimentally confirmed by rheology, light scattering, small angle neutron scattering and fluorescence.[4-10] When dissolving in a polar solvent, all phenomena related to the aggregation in nonpolar solvents disappear because of the dissociation of the ion-pairs. On the other hand, the study of the ionomers in aqueous media has attracted much less attention because of the poor solubility of its hydrophobic backbone in water. Recently, it has been found that randomly carboxylated and lightly sulfonated polystyrene ionomer chains can form stable colloidal nanoparticles in water if a dilute solution of an ionomer in tetrahydrofuran (THF) is added dropwise into an excessive amount of water.[11] Kutsumizu *et al.*[12] investigated the aggregate-water interface and the local mobility of aggregate inside.

In the present work, fluorescence together with laser light scattering were used to demonstrate that the polyethylene ionomers in which the ionic groups such as acrylate potassium salt, acrylamide, acrylic acid are introduced can form stable colloidal nanoparticles in water. The emphasis of this study will be on how the formation and structure of the stable nanoparticles depends on the kind of ionic groups.

Experimental Section

Modification of PE-7.6MA. The modification of poly(ethylene-*co*-methylacrylate) (PE-7.6MA), which contains 7.6 mol % methylacrylate, is carried out as described previously.[13] The weight-average molecular weight (M_w) and the number-average molecular weight (M_n) of PE-7.6MA were obtained from (GPC) (see Table 1). The mole fractions of the pendant ionic groups were calculated based on nitrogen analysis and the KOH amounts used in hydrolysis. Three modified ionomer samples were used in this study. The kind and content of the pendant ionic groups of these three samples are as follows: One of them [poly(ethylene-*co*-acrylate potassium salt)] contains 7.6 mol% acrylate potassium salts (designated as PE-7.6KAA hereafter). Another ionomer sample [poly(ethylene-*co*-acrylate potassium salt-*co*-acrylamide)] contains 3.8 mol% acrylate potassium salts and 3.8 mol% amide groups

Table 1. Molecular characteristics of parent polymer, PE-7.6MA

M_w	M_n	Polydispersity
203000	20900	9.7

(designated as PE-3.8KAA-3.8AM hereafter). The third ionomer sample [poly(ethylene-*co*-acrylate potassium salt-*co*-acrylic acid-*co*-acrylamide)] contains 2.3 mol% acrylate potassium salts, 1.5 mol% acrylic acids, and 3.8 mol% amide groups (designated as PE-2.3KAA-1.5AA-3.8AM hereafter).

Sample Preparation for Fluorescence Spectroscopy. Sample solutions were prepared by dilution with probe solution. All samples were ultrasonicated for at least 15 min to ensure a complete dispersion of the fluorescence probe molecules. Then, the solutions were allowed to stand at room temperature for at least 24 hours before the fluorescence measurements.

Sample Preparation of Solutions for Light Scattering. Cylindrical quartz cells of 12 mm diameter (Corning, USA) were used in all the light scattering experiments. The cells were soaked for 1 hour in concentrated sulfuric acid, rinsed with tap water. In series the cells were soaked in aqueous $NaOH/KMnO_4$ solution, rinsed with tap water, and finally rinsed thoroughly with distilled, deionized, and filtered water, and then steamed. Ionomer solutions were prepared by dilution of stock solutions. Solutions were filtered through a 0.22-μ Millipore filter directly into the light scattering cells.

Fluorescence Measurements. To examine the microenvironment of ionomer particles in aqueous media, fluorescence spectra were recorded on a Jasco FP-777 fluorescence spectrophotometer equipped with a thermoregulated cell compartment and with right-angle geometry (90 collecting optics). The temperature of the sample was controlled by a water circulator thermostat (JECO TECH MC11). Pyrene and 8-anilino-1-naphthalene-sulfonic acid (ANS) were used here as a fluorescence probe. They were purchased from Aldrich Chemical Co. and used as received.

The fluorescence excitation spectra of pyrene were recorded with the emission wavelength of 387 nm. The fluorescence emission spectra of pyrene were recorded with the excitation wavelength of the 334 or 339 nm. Both of the above measurements, the slit width was set at 1.5 nm for the excitation and 3 nm for the emission. The pyrene concentration of the sample was kept constant at 2.1 μM.

The fluorescence emission spectra of ANS were also recorded with the excitation wavelength of the 380 nm. The slit width was set at 10 nm for the excitation and 5 nm for the emission. The ANS concentrations of the sample was kept constant at 23 μM.

Dynamic Light Scattering. Dynamic light scattering (DLS) experiments were performed on a Brookhaven Instruments Corp. photon correlation spectrometer fitted with a Brookhaven Instruments BI-9000AT (version 6.03) digital correlator and a Melles Griot He/Ne laser, which operated at a power of 30 mW and supplied vertically polarized light with a wavelength of 632.8 nm. All experiments were performed at a temperature of 30 °C. The measured autocorrelation function was analyzed by the cumulant method.[14] The hydrodynamic radius of modified PE-7.6MA particle was calculated by the Stokes-Einstein equation. The constrained regularized continuous inversion (CONTIN) program was used in the ill-posed Laplace inversion of the intensity-intensity autocorrelation functions from DLS to obtain the size distribution.

Results and Discussions

Formation and Structure of the Ionomer Particles. Pyrene, as one of the most sensitive probes, has been widely used to study the association and micellization of macromolecules in solution. Because of the remarkable changes of its photochemical properties when it is transferred from a polar environment to a nonpolar one, an increase in the quantum yield and a change in the fine vibrational structure reflected in the intensity ratio (I_1/I_3) of the first and third bands in its emission spectrum may be compared.[15-19]

Figure 1 presents typical emission fluorescence spectra of pyrene in aqueous PE-7.6KAA dispersions above and below the critical micelle concentration (cmc). The two noteworthy features of these spectra are that the intensity increase with increasing ionomer concentration and that there are changes in the intensity ratio of the first and third vibrational bands, I_1/I_3. As seen in Figure 2, pyrene in water has a very small absorption at 339 nm, which increases substantially upon transfer to the less polar environment. It is the increase in light absorbed that makes the largest contribution to the intensity increase seen Figure 1. In addition, this increase in the intensity reflects the increase of the lifetime of the excited state of pyrene, which is significantly different for the different probe surroundings.[17,20]

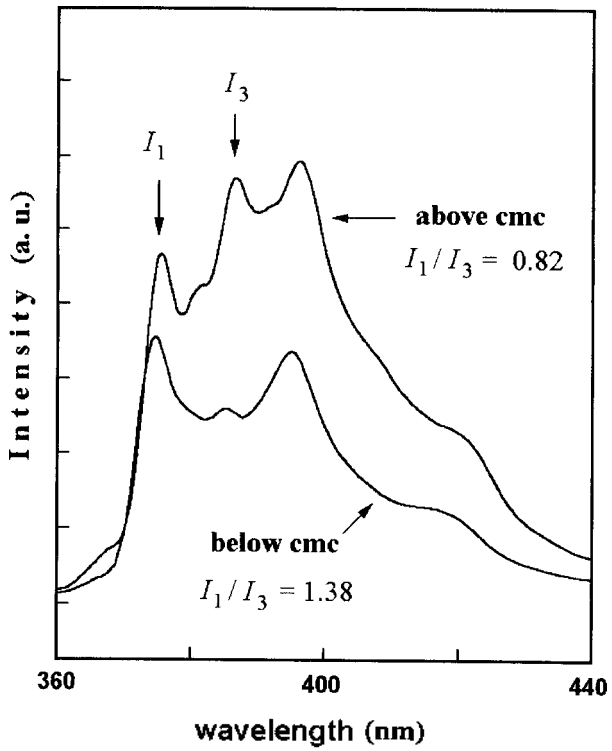

Figure 1. Pyrene fluorescence in aqueous PE-7.6KAA ionomer dispersions below and above cmc, λ_{ex}=339 nm.

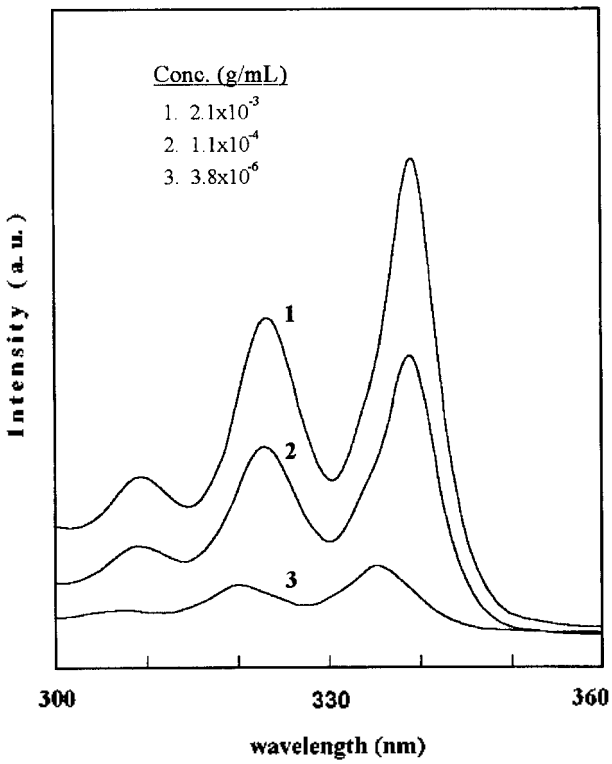

Figure 2. Excitation spectra of pyrene in aqueous dispersions of PE-7.6KAA ionomer at different concentrations, λ_{em}=387 nm.

In Figure 2, one can see a shift of (0,0) band from 335 to 339 nm. These changes accompany the transfer of pyrene molecules from water environment to the hydrophobic colloidal interior and thus provide information on the location of the pyrene probe in the system.

Figure 3 shows typical ionomer concentration dependence of the fluorescence intensity ratio of I_1/I_3 in the pyrene emission spectrum and ionomer concentration dependence of the wavelength shift of (0,0) band in the pyrene excitation spectrum. The intensity ratio (I_1/I_3) of pyrene is sensitive to the polarity of medium. According to Kalyanasundaram *et al.*,[20] the ratio can change from a value of ~1.9 in dimethyl sulfoxide to 0.5 in perfluoro-

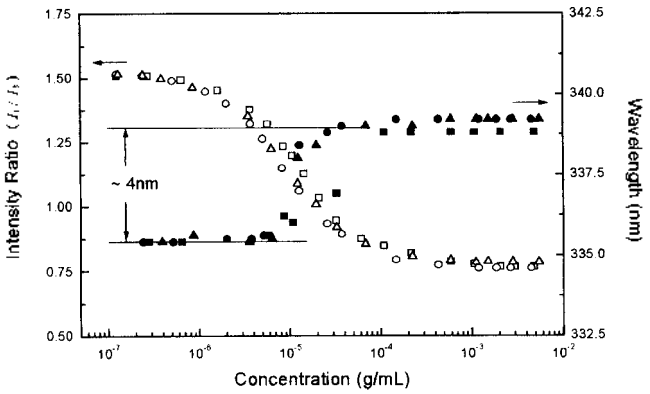

Figure 3. Ionomer concentration dependence of the intensity ratio (I_1/I_3) and (0,0) band absorption of pyrene in different ionomer dispersions. PE-7.6KAA (□, ■), PE-3.8KAA-3.8AM (○, ●), PE-2.3KAA-1.5AA-3.8AM (△, ▲).

methylcyclohexane and are thus helpful for determining the location of pyrene probe in the colloidal particles. They reported that its value is 1.52 in water and about 0.60 in hydrocarbon solvents. Figure 3 shows that the intensity ratio is ~1.5 when the ionomer concentration is extremely dilute, indicating that most of pyrene molecules are surrounded by water molecules. When the ionomer concentration is higher than $\sim 1\times10^{-6}$ g/mL, the ratio starts to decrease, very similar to the red shift of the (0,0) band absorption in the excitation spectra of pyrene, indicating the onset of ionomer aggregation and the partition of pyrene between water and the hydrophobic microdomain, *i.e.*, between inside and outside of the aggregates of the ionomer backbone chains. The turning point of I_1/I_3 curve is close to that of the wavelength of (0,0) band absorption. A plateau value of ~0.78 in the intensity ratio curve at the ionomer concentration higher than $\sim 1\times10^{-3}$ g/mL indicate the complete transfer of pyrene molecules from water to the hydrophobic environment of the colloidal particles. We calculated the cmc values on the onset of aggregation and the plateau values of the I_1/I_3 for three different ionomers. These values are presented in Table 2. The plateau values of the I_1/I_3 are slightly higher than ~0.60 measured in hydrocarbon solvents. From these results, we consider the microstructure of colloidal particles, which might still contain some captured water molecules and/or a small part of pendant ionic groups are remaining in the particle inside.

We found that all of the three modified PE-7.6MA ionomers in aqueous dispersions the (0,0) band of the S_2-S_0 absorption of pyrene is shifted ~4 nm to red in comparison with that in pure water, indicating the aggregation of the ionomer chains. Similarly to this, the red shift is ~5 nm in

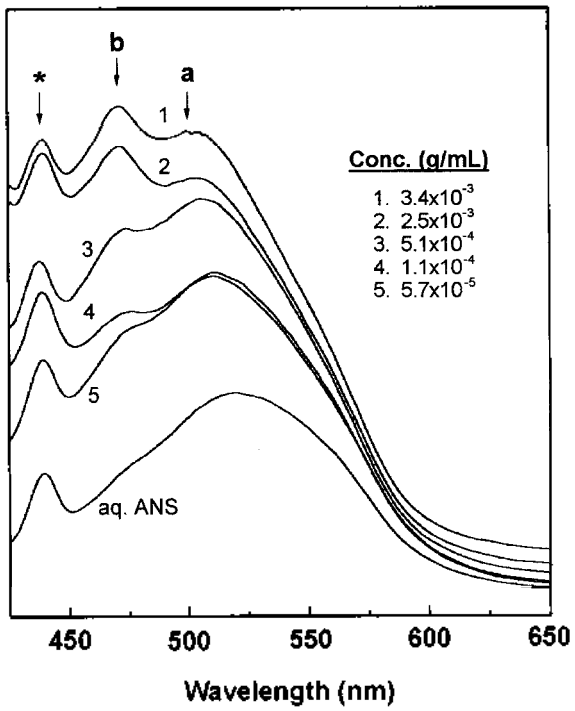

Figure 4. ANS emission spectra in aqueous PE-7.6KAA ionomer dispersions at various concentrations, λ_{ex}=380 nm. *: Raman scattering band of water vibrational mode, (a) and (b): emission band by binding and free ANS, respectively.

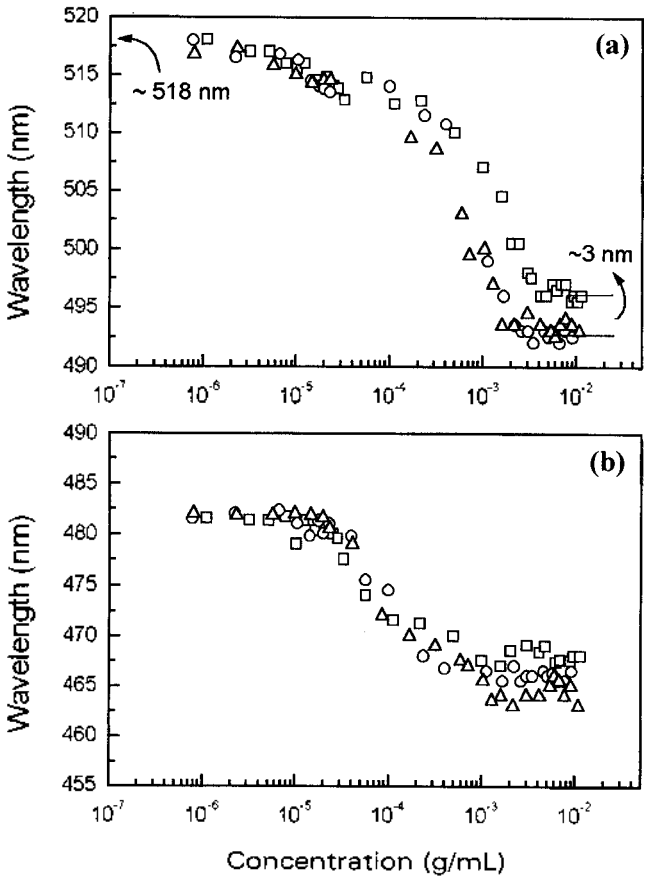

Figure 5. Ionomer concentration dependence of emission band of free ANS (a) and binding ANS (b) in different ionomer dispersions. PE-7.6KAA (□), PE-3.8KAA-3.8AM (○), PE-2.3KAA-1.5AA-3.8AM (△).

case of sodium sulfonated polystyrene ionomer particles[11] and 2-5 nm in case of a micelle system[15,17]

ANS (8-anilino-1-naphthalenesulfonic acid), an amphoteric probe, is selectively solubilized at water-hydrophobic interface.[21,22] In contrast to pyrene, the fluorescence spectra of solutions containing the ANS probe give the information of the environments of the polymer particles near surface in aqueous media.[21] The fluorescence emission maximum is shifted from 520 nm in aqueous environments to 462 nm in hydrophobic environments.[23-24]

As shown in Figure 4, we found two maxima peaks which are ~480 and ~515 nm in dilute ionomer concentrations, indicating that ANS experiences two different environment in ionomer solutions.[21,25-26] A shorter wavelength is due to ANS binding to the hydrophobic region of ionomer particles. On the other hand, a longer wavelength is attributed to both free ANS in bulk and ANS located near water-colloidal interface.

Figure 5(a) (for longer wavelength) and 5(b) (for shorter wavelength) show ionomer concentration dependence of the wavelength in ANS emission spectra. In Figure 5(a), when the ionomer concentration is very dilute, the wavelength of ANS is ~518 nm, very similar to that of ANS in water, indicating that most of ANS molecules are surrounded by water molecules. With increasing the ionomer concentration, the wavelength is shifted to blue. A plateau value in the

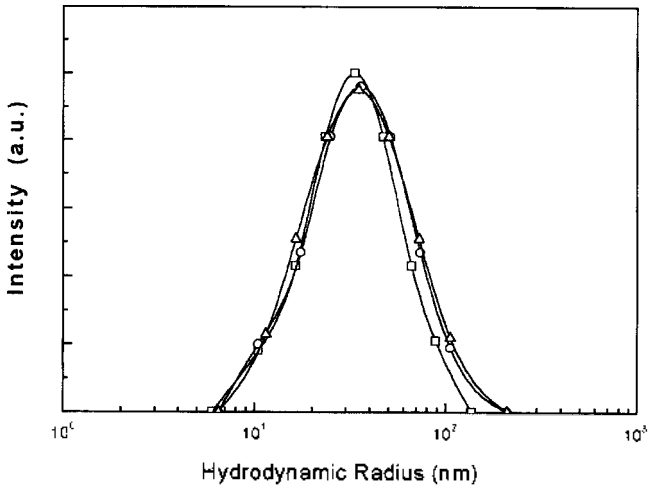

Figure 6. Particle size distributions at slightly above CMC in three different ionomer dispersions. PE-7.6KAA (□), PE-3.8KAA-3.8AM (○), PE-2.3KAA-1.5AA-3.8AM (△).

wavelength curve at the ionomer concentration higher than $\sim 2\times10^{-3}$ g/mL is different in three ionomers. The plateau value of PE-7.6KAA is slightly higher than that of the other two ionomers, indicating that the surface of colloidal particles made up PE-7.6KAA ionomers in aqueous media is relatively more polar than the other two ionomers. In Figure 5(b), when the ionomer concentration is very dilute, the wavelength of ANS is kept constant. When the ionomer concentration is higher than $\sim 1\times10^{-5}$ g/mL, the wavelength dramatically decreases, indicating the onset of aggregation. we also determined the cmc by crossover in Figure 5(b). These values for three different ionomers are presented in Table 2. The cmc values obtained by ANS fluorescence measurements are close to those obtained by pyrene fluorescence measurements. Kutsumizu *et al.* detected that the mobility of the ionomer chains was greatly restricted in a layer of thickness of 10 Å from the aggregate-solvent interface and the restricted mobility was attributed to constraints arising from the presence of proximal ionic groups in ethylene-methacrylic ionomers in aqueous solutions.[12] Thus the probe molecules located on the hydrophobic layer near the aggregate-solvent interface is restricted in mobility. Abrupt blue shift shown in Figure 5(b) is due to that ANS molecules strongly bind to colloidal hydrophobic site near interface and/or that the mobility of ANS probe molecules located on hydrophobic region near interface are restricted.

Size Distribution of Colloidal Nanoparticles. Dynamic light scattering as a powerful analytical tool can be used to directly determine the size distribution of the colloidal particles. Figure 6 shows typical apparent size distributions of the stable colloidal particles made of different modified PE-7.6MA ionomers. It clearly shows that the particles formed through the hydrophobic aggregation of the ionomers in water are very small in the nanometer range. From the second-order cumulant analysis, we found that the average hydrodynamic radius of the PE-7.6KAA, PE-3.8KAA-3.8AM, and PE-3.8KAA-3.8AM nanoparticles are 31, 38, and 38 nm, respectively. These indicates that the average particle size depends on the

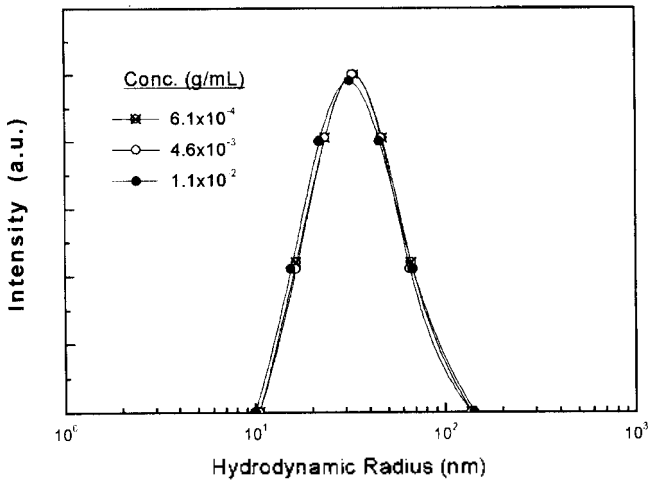

Figure 7. Hydrodynamic radius (R_H) distributions in aqueous PE-3.8KAA-3.8AM ionomer dispersions after forming the stable colloidal particles.

Table 2. Comparison of cmc values and plateau values in different ionomer dispersions

Ionomers	cmc ($\times 10^{-6}$ mg/mL)			plateau value		
	for pyrene		for ANS	for pyrene		for ANS
PE-7.6KAA	8.5[a]	4.9[b]	7.5[c]	0.77[d]	338.8[e]	496.3[f]
PE-3.8KAA-3.8AM	3.0	4.6	6.5	0.76	339.2	492.7
PE-2.3KAA-1.5AA-3.8AM	2.8	3.8	6.0	0.78	339.2	493.3

[a] and [b] the crossover concentration determined from the intensity ratio (I_1/I_3) and the (0,0) band absorption data of pyrene, respectively. [c] the crossover concentration determined from the emission band of binding ANS. [d] Intensity ratio (I_1/I_3). [e] Wavelength (nm) of (0,0) band absorption. [f] Emission wavelength (nm) of free ANS.

pendant ionic salt content, namely, the higher the ionic salt content, the smaller the average particle size, which agrees well with previous study of the carboxylated ionomers and sulfonated polystyrene ionomers.[11] Figure 7 shows a successive dilution of the PE-3.8KAA-3.8AM dispersion in the range of 6.1×10^{-4}~1.1×10^{-2} g/mL has nearly no effect on the particle size distribution. This indicates the effect of the ionic interaction on the measured particle size distribution is not significant. Otherwise, the increase of the interparticle distance due to the dilution will decreases the ionic interaction and affect the measured size distribution. On the other hand, Figure 7 shows that the nanoparticles stabilized by the ionic groups on the surface are very stable and they are very different from simple aggregation, namely there is no equilibrium between individual chains and particles. This fact is strongly supported by the TEM of ionomers used in this study (Figure 8).

It should be noted that it is difficult to determine the particle size distribution for such small nanoparticles when the concentration is lower than ~10^{-5} g/mL. In contrast, the intensity ratio of I_1/I_3, and wavelength change show substantial variations over the same concentration. A combination of the DLS and fluorescence results leads us to the following picture: it is realized that the hydrophobic

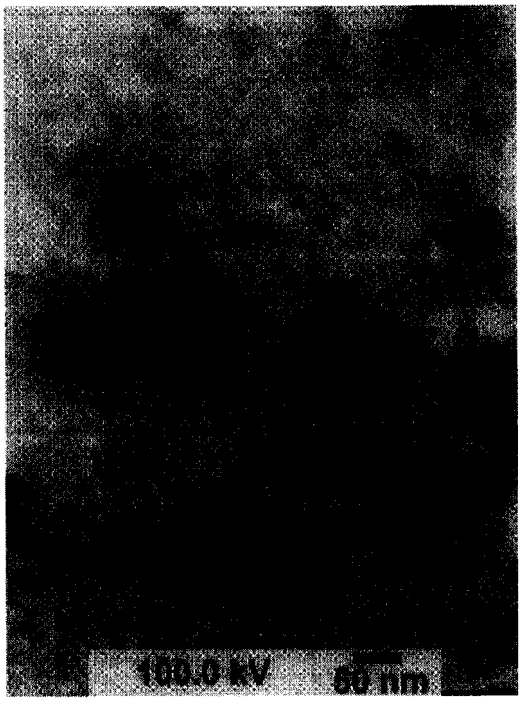

Figure 8. Transmission electron micrograph showing PE-3.8KAA-3.8AM ionomer particles. The scale bar on the micrograph prints shows 50 nm.

ethylene backbone chains in aqueous modified PE-7.6MA ionomer solution start to aggregate at very low cmc and stabilize its nanoparticle formation with narrow range distribution, in which the ionic groups have a tendency to stay at the surface of the interchain aggregates.

Conclusion

Ionomers which is modified by hydrolysis and/or ammonolysis of poly(ethylene-*co*-methylacrylate) can form surfactant-free nanoparticles in aqueous solution. The nanoparticles stabilized by the electrostatic repulsion between the ionic groups on different particles are very stable and they are very different from simple aggregation, namely there is no equilibrium between individual chains and particles. The environment of colloidal particles inside might still contain some captured water molecules and/or a small part of pendant ionic groups. The particle size distribution is strongly dependent on the kind of pendant ionic groups, but nearly independent on the ionomer concentrations after forming the stable nanoparticles. We believe that our results have provided a convenient way to study the formation and structure of surfactant-free colloidal nanoparticles stabilized by ionic groups on the particle surface.

This study demonstrate another way to prepare surfactant-free nanoparticles that could be used to encapsulate or carry hydrophobic drugs or other hydrophobic molecules for different applications.

Acknowledgment. This work was partially supported by S.N.U. Posco Research Fund (97-05-2078). Authors are very much indebted to Dr. Jae Heung Lee and Dr. Kil-Yeong Choi of Korea Research Institute of Chemical

Technology for their helpful discussion throughout this studies.

References

1. Mauritz, K. A. In *Structure and Properties of Ionomers*; Pineri, M.; Eisenberg, A. Eds.; NATO ASI Series; D. Reidel Publishing: Dordrecht, Holland, 1987; p 11.
2. Otocka, E. P. *J. Macromol. Sci. Revs. Macromol. Chem.* **1971**, *C5*, 275.
3. Lundberg, R. D.; Makowski, H. S. *J. Polym. Sci., Part B-Polym. Phys.* **1980**, *18*, 1821.
4. Lantman, C. W.; MacKnight, W. J.; Peiffer, D. G.; Sinha, S. K.; Lundberg, R. D. *Macromolecules* **1987**, *20*, 1096.
5. Ermi, B. D.; Amis, E. J. *Macromolecules* **1996**, *29*, 2701.
6. Gabrys, B.; Higgins, J. S.; Lantman, C. W.; MacKnight, W. J.; Pedley, A. M.; Peiffer, D. G.; Rennie, A. R. *Macromolecules* **1989**, *22*, 3746.
7. Pedley, A. M.; Higgins, J. S.; Peiffer, D. G.; Burchard, W. *Macromolecules* **1990**, *23*, 1434.
8. Dowling, K. C.; Thomas, J. K. *Macromolecules* **1991**, *24*, 4123.
9. Bakeev, K. N.; MacKnight, W. J. *Macromolecules* **1991**, *24*, 4578.
10. Bakeev, K. N.; Teraoka, I.; MacKnight, W. J.; Karasz, F. E. *Macromolecules* **1993**, *26*, 1972.
11. Li, M.; Jiang, M.; Wu, C. *J. Polym. Soc., Part B-Polym. Phys.* **1997**, *35*, 1593.
12. Kutsumizu, S.; Schlick, S. *Macromolecules* **1997**, *30*, 2329.
13. Lee, J. H.; Choi, K. Y.; Seoh, G. B.; Min, B. K.; Yoon, S. *Polymer(Korea)* **1997**, *21*, 575.
14. Koppel, D. E. *J. Chem. Phys.* **1972**, *57*, 4814.
15. R. Zana, In *Surfactant Solutions: New Methods of Investigation*; R. Zana, Ed.; Marcel Dekker: New York, U. S. A. 1986; p 241
16. Wang, Y.; Winnik, M. A. *Langmuir* **1990**, *6*, 1437.
17. Wilhelm, M.; Zhao, C. L.; Wang, Y.; Xu, R.; Winnik, M. A. *Macromolecules* **1991**, *24*, 1033.
18. Yekta, A.; Duhamel, J.; Brochard, P.; Adiwidjaja, H.; Winnik, M. A. *Macromolecules* **1993**, *26*, 1829.
19. Astafieva, I.; Zhong, X. F.; Eisenberg, A. *Macromolecules* **1993**, *26*, 7339.
20. Kalyanasundaram, K.; Thomas, J. K. *J. Am. Chem. Soc.* **1977**, *99*, 2039.
21. Ikemi, M.; Odagiri, N.; Tanaka, S.; Shinohara, I.; Chiba, A. *Macromolecules* **1982**, *15*, 281.
22. Stryer, L. *J. Mol. Biol.* **1965**, *13*, 482
23. Branham, K. D.; Middleton, J. C.; McCormick, C. L. *Polymer preprints* **1991**, *32*(1), 106.
24. Yang, H.; Zhong, H. *Biochem. Mol. Bio. Int.* **1997**, *41*(2), 257. references therein.
25. Dutta, S.; Maiti, N. R.; Bhattacharyya, D. *Eur. J. Boichem.* **1997**, *244*, 407.
26. Aubin, L. B.; Lissi, E. A.; Aspee, A.; Gonzalez, F. D.; Varas, J. M. *J. Colloid Interface Sci.* **1997**, *186*, 332.

Synthesis of 10-Oxo-β-rhodomycinone Derivatives

Young S. Rho*, Sun Y. Kim, Inho Cho, Heun Soo Kang, Dong Jin Yoo†, and Chaejoon Cheong‡

Department of Chemistry, Chonbuk National University, Chonju 561-756, Korea
†Department of Chemistry, Seonam University, Namwon 590-170, Korea
‡Magnetic Resonance Group, Korea Basic Scienece Institute, Taejon 305-333, Korea
Received June 8, 1998

Regiospecific total syntheses of (±)-11-deoxy-4-methoxy-10-oxo-β-rhodomycinone (**21a**) and (±)-11-deoxy-1-methoxy-10-oxo-β-rhodomycinone (**21b**) are described. 2-(2-Bromoethyl)-1,3-dioxane (**6**) was transformed to naphthalenone **12**, which was condensed with (phenylsulfonyl)-isobenzofuranone **13** to afford 7,8-dihydro-9-ethyl-6-hydroxy-4-methoxynaphthacen-5,12-dione (**15**). Epoxide **16** prepared from olefinic compound **15**, reacted with HF/Pyr (7 : 3) to give **17**. Dihydroxylation of **17** with *t*-BuOK/$P(OMe)_3/O_2$, selective *cis*-diol protection of mixed compounds **18** with phenylboronic acid in toluene, separation of *cis*-boronate **19** and *trans*-diol **20** by column chromatography on silica gel, and cleavage of the boronate group of **19** with 2-methylpentane-2,4-diol in acetic acid completed the construction of **21**.

Introduction

Rhodomycins in anthracycline series were first discovered by Krassilnikov and Koreniakov.[1] Among these, rhodomycin and isorhodomycin family produced by *streptomyces purpurascens* were the first anthracycline compounds whose structures were elucidated by Brockmann and coworkers.[2] Rhodomycins like daunomycin and aklavin are well-known, clinically useful anticancer chemotherapeutic agents against acute leukemia and human cancer, as well as various experimental tumors. Since then, anthracyclines have been the objects of intensive clinical tests and synthetic studies for the last decade because of their strong antineoplastic activities.[3] Numerous synthetic approaches have been